Aerosol and Air Quality Research, 13: 1404–1410, 2013

ISSN: 1680-8584 print / 2071-1409 online
doi: 10.4209/aaqr.2013.05.0144

The Predictive Method for the Submicron and Nano-Sized Particle Collection Efficiency of Multipoint-to-Plane Electrostatic Precipitators

Thi-Cuc Le, Guan-Yu Lin, Chuen-Jinn Tsai*

Institute of Environmental Engineering, National Chiao Tung University, No.1001 University Road, Hsin Chu, 300, Taiwan

ABSTRACT

The multipoint-to-plane electrostatic precipitator (ESP) is one type of ESP devices used for the sampling and control of nanoparticles and sub-micron particles, with the advantage of a low pressure drop and high particle collection efficiency. Several empirical equations for predicting the particle collection efficiency are available in the literature, but most of them are only applicable to wire-in-plate ESPs. For ESPs with different discharge electrodes, the empirical equations are different since the ion concentration and electric fields are different. In this paper, a predictive method is developed to calculate the particle migration velocity and the particle collection efficiency equation $\eta(\%)$ of multipoint-to-plane ESPs in the form of $\eta(\%) = \{1 - \exp\{-[\beta_1(N_{De}^{\beta_2}) + \beta_3(N_{De}) + \beta_4]\}\} \times 100\%$, in which β_1, β_2, β_3 and β_4 are regression coefficients and N_{De} is the Deutsch number determined by the particle migration velocity. Good agreement is obtained between the present model predictions and the experimental particle collection efficiencies obtained from the literature. It is expected that the present model can be used to facilitate the design of efficient multipoint-to-plane ESPs for nanoparticle and sub-micron particles removal in the future.

Keywords: Multipoint-to-plane ESPs; V-I characteristic; Deutsch-Anderson equation; Particle control.

INTRODUCTION

Because of low pressure drop and high particle collection efficiency, electrostatic precipitators (ESPs) are widely used in the industry to remove particles suspended in the exhaust gas (Ruttanachot *et al.*, 2011), in which the wire-to-plate ESP is the most commonly used. The multipoint-to-plane ESP, whose schematic diagram is shown in Fig. 1 is the other design type which has a low corona onset voltage and good resistance to mechanical shock and is often used in applications such as ozone generation and exhaust gas cleaning (Dasculescu *et al.*, 1999). It is also used to enhance the particle collection efficiency of stainless steel (SS) filters (Kim *et al.*, 2000; Mermelstein *et al.*, 2002) and to sample particles (Sillanpää *et al.*, 2008).

When a high voltage is applied to the point electrode in the multipoint-to-plane ESP, ionization, attachment and recombination between air ions and particles occur in a thin layer around the tip of the electrode, which is called the ionization region. The area outside the ionization region is called the drift region, in which unipolar charged ions with the same polarity as the discharge electrode are drifted to the grounded electrode and ion current is generated (Adamiak *et al.*, 2005). The tips of the point discharge electrodes generate higher electric filed and current density than those in the wire-to-plate ESP, which lead to higher particle collection efficiency (Lin *et al.*, 2012b).

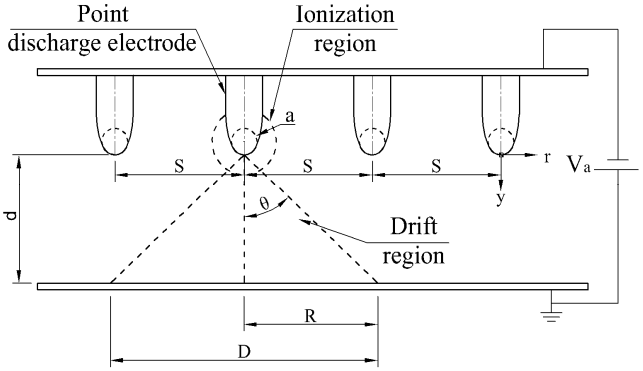

Fig. 1. The schematic diagram of a multipoint-to-plane ESP.

Multipoint-to-plane ESPs has been studied for the current density distribution (Dascalescu *et al.*, 1999), the V-I characteristic (Thanh, 1985; El-Mohandes *et al.*, 1999; Kazlov and Solovyov, 2005) and particle collection efficiency (Kim *et al.*, 2000; Huang and Chen, 2001; Mermelstein *et al.*, 2002; Sillanpää *et al.*, 2008; Kim *et al.*, 2012). The particle collection efficiency of multipoint-to-plane ESPs

* Corresponding author.
Fax: +886-3-5731880
E-mail address: cjtsai@mail.nctu.edu.tw

was found to increase with an increasing particle residence time (Kim *et al.*, 2000), an increasing applied voltage (Huang and Chen, 2001), an increasing length of the collection electrode, an increasing number of discharge electrodes and a decreasing gap spacing between the tip of the discharge and collection electrodes (El-Mohandes *et al.*, 1999; Brocilo, 2003; Kazlov and Solovyov, 2005). However, only experimental data are presented in the previous literature for the collection efficiency. No mathematical models to explain the data are readily available, which are important to the design and scale-up of the efficient multipoint-to-plane ESPs. In this study, a modified Deutsch-Anderson equation based on the work of Lin *et al.* (2013) is used to predict the collection efficiencies of multipoint-to-plane ESPs for nanoparticles and submicron particles and then the predictions are validated by previous experimental data of Kim *et al.* (2000) and Mermelstein *et al.* (2002).

PRESENT MODEL

The theoretical particle collection efficiency for the ESP is the following well-known Deutsch-Anderson derived which is based on many ideal assumptions (Matts and Öhnfeldt, 1964):

$$\eta(\%) = [1 - \exp(-N_{De})] \times 100\% \tag{1}$$

where N_{De} is the Deutsch number which can be calculated as:

$$N_{De} = \frac{WA}{Q} \tag{2}$$

where A is the area of the collection electrode (m^2), Q is the air flow rate (m^3/s), and W is the particle migration velocity (m/s). The Matts-Ohnfield equation (M-O) is a modified Deutsch-Anderson equation in which an additional exponent, k_1, which ranges from 0.4 to 0.6, is used to provide a more conservative estimate of the removal efficiency (Matts and Öhnfeldt, 1964):

$$\eta(\%) = \{1 - \exp[-(N_{De})^{k_1}]\} \times 100\% \tag{3}$$

Another modified Deutsch-Anderson equation was developed by Lin *et al.* (2013) to calculate the particle collection efficiency of a wet-electrocyclone in which saw-type discharge electrodes are used:

$$\eta(\%) = \{1 - \exp\{-[\beta_1 (N_{De}{}^{\beta_2}) + \beta_3 (N_{De}) + \beta_4]\}\} \times 100\% \tag{4}$$

where the regression coefficients are 6.122 for β_1, 0.7289 for β_2, –3.273 for β_3, and 0.5821 for β_4. This equation will be used in this study to predict the particle collection efficiency of the multipoint-to-plane ESP as it has multiple sharp-point discharge electrodes similar to the saw-type electrodes in the electrocyclone of Lin *et al.* (2013). To use Eq. (4) to calculate the collection efficiency, the particle migration velocity is needed. The method to calculate the particle migration velocity for determining the collection efficiency is the main focus of this study.

Particle Migration Velocity

The particle migration velocity (m/s) can be calculated as (Lin *et al.*, 2012a):

$$W = \frac{n_p(t) e E_{ave} C(d_p)}{3\pi\mu d_p} \tag{5}$$

where d_p is the particle diameter (m), $C(d_p)$ is the slip correction factor for the particle with the diameter d_p, μ is the air dynamic viscosity (N-s/m^2), $n_p(t)$ is the total number of elemental units of charge (#) as a function of particle charging time (or the resident time of particles in the ESP) t (sec), e is the elementary charge (C), and E_{ave} is the average electric field strength (V/m) given by:

$$E_{ave} = \frac{\int_0^d E_y(y)\,dy}{d} \tag{6}$$

in which d is the point-to-plane spacing (m) and the axial electric field distribution from the tip to the collection electrode, $E_y(y)$ (V/m), is given by (Abdel-Salam *et al.*, 2007):

$$E_y(y) = \frac{2V_a}{\ln\left(\frac{4d}{a}\right)} \frac{1}{2y + a - \frac{y^2}{d}} \tag{7}$$

where V_a is the applied voltage (V), a is the tip radius of discharge electrode (m), and y is the distance from the tip of discharge electrode (m).

The particle electrostatic charge as a function of time, $n_p(t)$ (#, number of elementary units of charges), is given by (Lin *et al.*, 2012a):

$$n_p(t) = n_{diff}(t) \times \exp\left[\delta_1 n_{diff}(t)^{\delta_2} + \delta_3 n_{diff}(t) + \delta_4\right] + n_{field}(t) \tag{8}$$

where

$$n_{diff}(t) = \frac{d_p kT}{2K_E e^2} \ln\left(1 + \frac{\pi K_E d_p \bar{c}_i e^2 N_i t}{2kT}\right) \tag{9}$$

$$n_{field}(t) = \left(\frac{3\varepsilon}{\varepsilon + 2}\right)\left(\frac{E_{ave} d_p{}^2}{2K_E e}\right)\left(\frac{\pi K_E e Z_i N_i t}{1 + \pi K_E e Z_i N_i t}\right) \tag{10}$$

In the above equations, δ_1 is 1.91588, δ_2 is –0.1425, δ_3 is 1.296×10^{-5}, and δ_4 is –1.2671, $\bar{c}_i$ is the mean thermal speed of ion (m/s), ε is the relative permittivity of the

particle, k is the Boltzmann constant (1.38×10^{-23} J/K), K_E is the constant of proportionality (9.0×10^9 N-m/C^2), and N_i is the average ion concentration (#/m^3) which can be determined as follows (Lin *et al.*, 2012a):

$$N_i = \frac{I_t}{AZ_i E_{ave} e} \tag{11}$$

where A is the drift region on the plane (m^2), and I_t, the total ion current (A), can be calculated as follows (Kazlov and Solovyov, 2005):

$$I_t = N \times I \tag{12}$$

where N is the number of point discharge electrodes, I is the ion current of a single electrode (A) which can be calculated as follows (Adamiak and Atten, 2004):

$$I = \alpha_i \varepsilon_0 Z_i V_a \left(V_a - V_0\right) / d \tag{13}$$

In the above equation, ε_0 is the gas permittivity (C^2/N-m^2), Z_i is the ion mobility (m^2/V-s), and V_0 is the breakdown voltage (V), and α_i is the empirical coefficient which can be obtained by the following equation:

$$\alpha_i = \gamma_1 \left(\frac{S}{d}\right)^{\gamma_2}, \; 0.28 \le \alpha_i \le 2.1 \tag{14}$$

where S is the point-to-point spacing (m) and γ_1 and γ_2 are regression coefficients which are 1.16 and 0.55, respectively, obtained in this work by fitting Eq. (14) to the experimental data of El-Mohandes *et al.* (1992), in which the *S/d* ratio ranges from 0.074 to 3.

The breakdown voltage is expressed as (Adamiak and Atten, 2004):

$$V_0 = \frac{E_s \times a \times \ln\left(\frac{4d}{a}\right)}{2} \tag{15}$$

in which the breakdown electric filed (V/m) is :

$$E_S = 3.1 \times 10^6 \, \delta \left(1 + \frac{0.308}{\sqrt{0.5 a \delta}}\right) \tag{16}$$

where a is in cm, and the constant δ is

$$\delta = \frac{T_0 P}{T P_0} \tag{17}$$

where P_0 is the standard pressure (bar), T is the air temperature (°K), and T_0 is the standard temperature (°K).

The circular drift region, A (m^2) can be calculated from the radius of the drift region on the collection electrode surface, R (m), as $A = \pi R^2$, where R can be determined as (Sigmond, 1985; Allibone *et al.*, 1993):

$$R = d \times \tan\theta \tag{18}$$

where

$$\tan\theta = \left\{ \left[1 - \frac{\alpha_i (m-2)}{2\pi} \right]^{\left(\frac{2}{2-m}\right)} - 1 \right\} \tag{19}$$

in which m is the Warburg's parametric index for the cosine power law, which is 4.82 for positive and 4.65 for negative corona, and θ is semi-apex angle of corona discharge (Allibone *et al.*, 1993).

Calculation Procedure

Fig. 2 shows the calculation procedure for the average electric field, ion current, particle migration velocity and particle collection efficiency in the present model. The empirical coefficient (α_i) and the breakdown voltage (V_0) are first obtained from Eq. (14) and Eqs. (15–17), respectively. Then the total ion current (I_t) and the drift region on the plane (A) are then calculated by Eqs. (12–13) and Eqs. (18–19), respectively while and the average electric field (E_{ave}) are calculated by Eqs. (6–7) followed by the calculation of the ion concentration (N_i) by Eq. (11). Subsequently, the particle electrostatic charge ($n_p(t)$) are obtained by Eqs. (8–10). The particle migration velocity (W) is then calculated by Eq. (5) and then the Deutsch number (N_{De}) is obtained by Eq. (2). Finally, the particle collection efficiency in the multipoint-to-plane ESP is calculated by using Eq. (4).

RESULTS AND DISCUSSION

Voltage-Current Characteristic

Fig. 3 shows the fitted curve obtained by fitting Eq. (14) to the experimental data of El-Mohandes *et al.* (1992) resulting in the regression coefficients of 1.16 for γ_1 and 0.55 for γ_2. Based on these regression coefficients, the total ion current (I_t) were calculated by Eq. (12) for different applied voltages (V_a). The calculated V-I curves compare very well with the experimental data of El-Mohandes *et al.* (1992) with six sewing needles (N = 6, a = 13–17 μm) and the point-to-plane spacing (d) and point-to-point spacing (S) ranging from 2.7–6.9 cm and 0.5–8.0 cm, respectively. Figs. 4(a) and 4(b) show only two examples for the comparison of the V-I curves between the present model predictions and the experimental data with d = 5 cm, S = 0.5, 2, 4, 6, and 8 cm and V_a = –5 to –26 kV for negative corona (Fig. 4(a)) and V_a = +5 to +19 kV positive corona (Fig. 4(b)). The deviation of the predicted total ion current from the experimental data is less than ± 20% when the negative ion mobility value of 2.3×10^{-4} m^2/V-s suggested by Adamiak and Atten (2004) is used (Fig. 4(a)), and is less than ± 21% when the positive ion mobility value of 1.4×10^{-4} m^2/V-s suggested by Lin and Tsai (2010) is used (Fig. 4(b)).

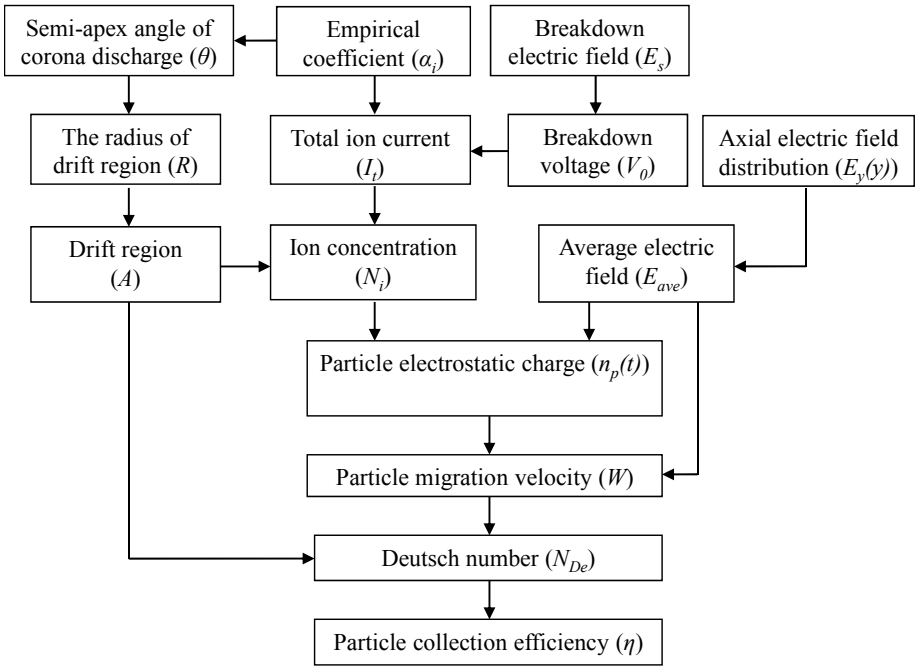

Fig. 2. The calculation procedure for the particle collection efficiency of multipoint-to-plane ESPs.

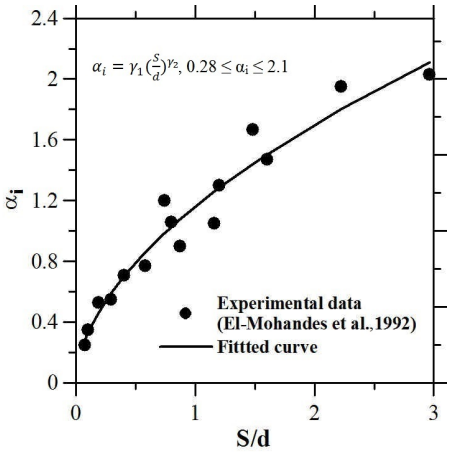

Fig. 3. The relationship between α_i and S/d.

The predicted V-I curves also agree with the experimental data of Thanh (1985) as shown in Fig. 5 for the multipoint-to-plane ESP with three needle-type discharge electrodes (a = 10 μm), the point-to-point spacing (S) of 2 cm, and the point-to-plane spacing (d) of 1.0–1.5 cm. Good agreement is obtained with a deviation of ± 18% when the applied voltage (V_a) ranges from –5 to –29 kV and the ion mobility is 2.3×10^{-4} m^2/V-s for negative ions (Adamiak and Atten, 2004). The above results suggest that Eq. (12) can be used to predict the ion current of the multipoint-to-plane ESPs with needle-type discharge electrodes with a good accuracy.

Particle Collection Efficiency

The regression coefficients of 6.122 for β_1, 0.7289 for β_2, –3.273 for β_3, and 0.5821 for β_4 are obtained from Lin *et al.* (2013) for N_{De} range of 0.13 to 4.69 and the particle electric mobility diameter range of $22.1 \le d_p \le 805.8$ nm.

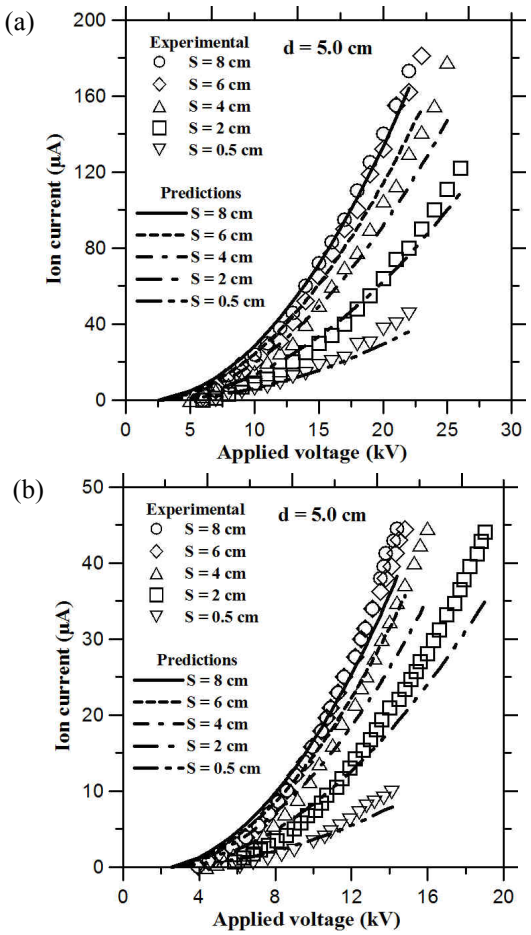

Fig. 4. The comparison of V-I curves between the present predictions and the experimental data of El-Mohandes *et al.* (1985) with d = 5 cm. (a) negative corona. (b) positive corona.

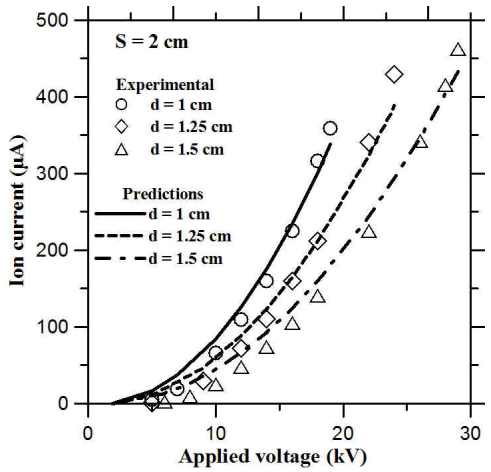

Fig. 5. The comparison of V-I curve between the present predictions and the experimental data of Thanh (1985).

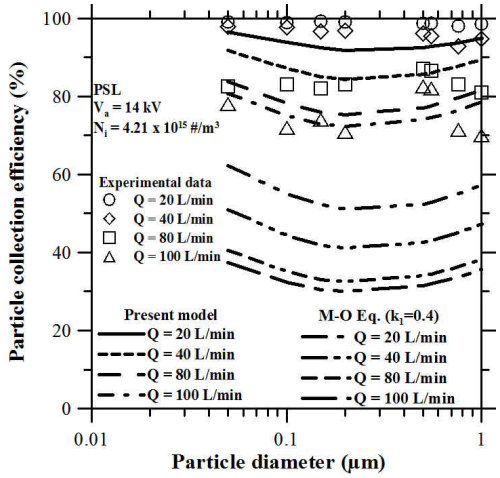

Fig. 6. The comparison of predicted particle collection efficiencies with the experimental data of Kim *et al.* (2000) for PSL particles.

The comparison of predicted particle collection efficiencies by the present model and the experimental data of Kim *et al.* (2000) are shown in Fig. 6 for polystyrene latex (PSL) particles with $0.05 \le d_p \le 1$ μm at the fixed applied voltage of +14 kV and the air flow rate ranging from 20 to 100 L/min. The multipoint-to-plate ESP used a fibrous SS filter as the grounded electrode (pore size: 20 μm). The predicted values agree reasonably with experimental data with a deviation of 2.68–7.9% at 20 L/min, 5.81–14.98% at 40 L/min, 0.81–12.91% at 80 L/min and 2.62–11.36% at 100 L/min when the positive ion mobility is 1.4×10^{-4} m^2/V-s (Lin and Tsai, 2010). In comparison, the deviation of particle collection efficiencies calculated by the M-O equation (k_1 = 0.4) from the experimental data at 20 L/min, 40 L/min, 80 L/min and 100 L/min is much larger, which is 37.17–48.44%, 47.95–57.52%, 50.83–60.86% and 49.14–61.82%, respectively. If the Deutsch-Anderson equation is used (or k_1 = 1.0 in the M-O equation), even a larger deviation occurs (data are not shown).

Figs. 7(a)–(c) show the comparison of predicted particle collection efficiencies with the experimental data of Mermelstein *et al.* (2002) for the multipoint-to-plate ESP with the fibrous and the porous SS filters with the pore size of 20 μm as grounded electrodes at the aerosol flow rate of 10 L/min, 20 L/min and 50 L/min, respectively. The test particles were NaCl with $0.03 \le d_p \le 1.0$ μm and the

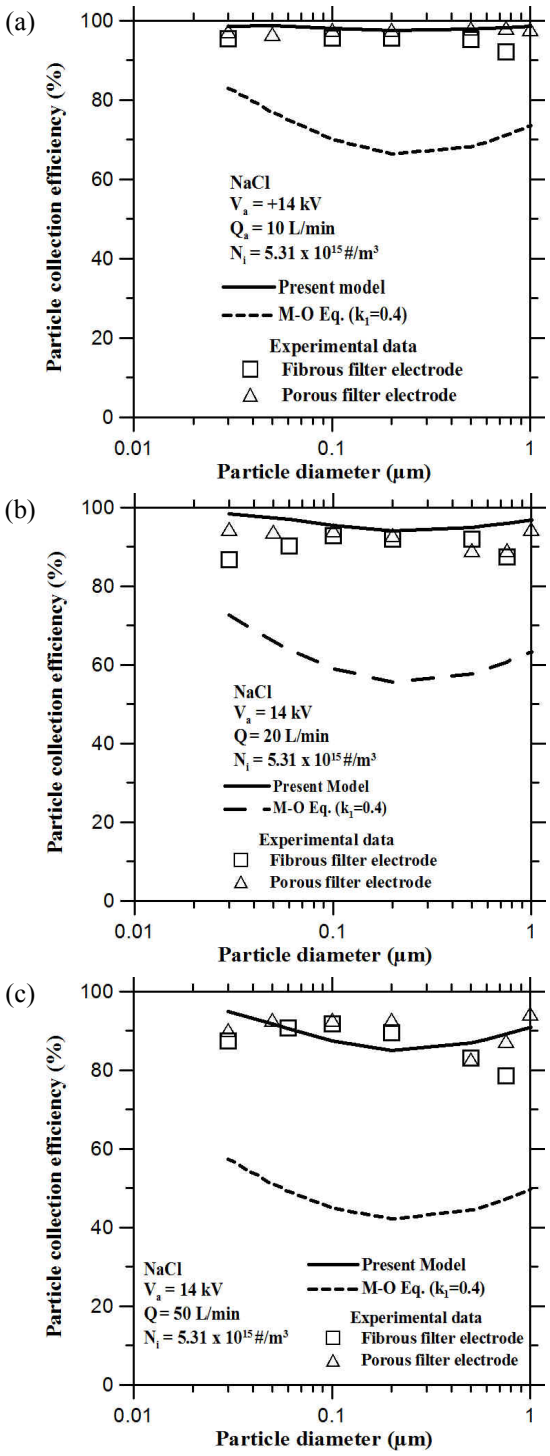

Fig. 7. The comparison of predicted particle collection efficiencies with the experimental data of Mermelstein *et al.* (2002) for NaCl particles at the aerosol flow rate of (a) 10 L/min (b) 20 L/min and (c) 50 L/min.

applied voltage was +14 kV. The data also refer to the ESP efficiencies only, which are obtained from the original figures of Mermelstein *et al.* (2002) who showed both the filtration efficiencies of the filters and total combined efficiencies of the ESP and the filters. The predictions are seen to agree well with the experimental data with a deviation of 2.3–6.52% at 10 L/min (Fig. 7(a)), 2.71–12.12% at 20 L/min (Fig. 7(b)) and 0.19–12.27% at 50 L/min (Fig. 7(c)) for the fibrous filter electrodes. For the porous SS electrodes, the deviation is smaller, which is 0.09–1.72% (10 L/min, Fig. 7(a)), 1.51–7.47% (20 L/min, Fig. 7(b)) and 1.97–8.5% (50 L/min, Fig. 7(c)). The reason why the agreement is better for the porous SS electrodes as compared to the fibrous SS electrodes is not known but is suspected to be due to smoother surface and more uniform electric field of the former than the later, which deserves further investigation in the future. Similar agreement between model predictions and experimental data are also obtained for the fibrous and porous filter grounded electrodes of other pore sizes (6, 7 and 16 μm-fibrous, 40 and 100 μm-porous) (data are not shown).

The deviation of the particle collection efficiencies calculated by the M-O equation ($k_1 = 0.4$) and the experimental data at the flow rate of 10 L/min, 20 L/min and 50 L/min is again larger, which is 13.07–30.51%, 16.20–39.51% and 34.32–52.87% for fibrous SS filters, respectively, and 36.33–54.52%, 32.18–40.26% and 36.33–47.13% for the porous SS filters, respectively. If the Deutsch-Anderson equation is used (or $k_1 = 1.0$ in the M-O equation), again even a larger deviation occurs (data are not shown).

CONCLUSIONS

This study developed a predictive model to calculate the particle migration velocity and particle collection efficiency of the multipoint-to-plane ESP for nanoparticles and submicron particles. The particle migration velocity is first calculated based on the empirical voltage-current relationship and particle electrostatic charge, and then the particle collection efficiency equation is calculated as $\eta(\%) = \{1 - \exp\{-[\beta_1(N_{De}{}^{\beta_2}) + \beta_3(N_{De}) + \beta_4]\}\} \times 100\%$ in which regression coefficients $\beta_1 = 6.221$, $\beta_2 = 0.7289$, $\beta_3 = -3.273$, and $\beta_4 = 0.5821$ and N_{De} is the Deutsch number ranging from 0.13–4.69. Good agreement is obtained with a deviation smaller than 20% between the predicted collection efficiencies and the experimental data in the literature. The present model is able to facilitate the design and scale-up efficient multipoint-to-plane ESPs for controlling emissions of nanoparticles as well as sub-micron particles. Future study can be aimed at investigating the particle loading effect of different materials on the collection efficiency and conducting field validation of the present model using a pilot-scale ESP.

ACKNOWLEDGEMENT

The authors would like to express their gratitude to the Taiwan National Science Council for financial support under contract number (NSC 99-2221-E-009 -038 -MY3).

REFERENCES

Abdel-Salam, M., Nakano, M. and Mizuno, A. (2007). Electric Fields and Corona Currents in Needle-to-Meshed Plate Gaps. *J. Phys. D: Appl. Phys.* 40: 3363–3370.

Adamiak, K. and Atten, P. (2004). Simulation of Corona Discharge in Point-Plane Configuration. *J. Electrostat.* 61: 85–98.

Adamiak, K., Atrazhev, V. and Atten, P. (2005). Corona Discharge in the Hyperbolic Point-Plane Configuration: Direct Ionization Criterion versus Approximate Formulations. *IEEE Trans. Dielectr. Electr. Insul.* 12: 1025–1034.

Allibone, T.E., Jones, J.E., Saunderson, J.C., Taplamacioglu, M.C. and Waters, R.T. (1993). Spatial Characteristics of Electric Current and Field in Large Direct-Current Coronas. *Proc. R. Soc. London, Ser. A* 441: 125–146.

Brocilo, D. (2003). Electrode Geometry Effects on the Collection Efficiency of Submicron and Ultrafine Dust Particles in Wire-Plate Electrostatic Precipitators, PhD Dissertation, McMaster University.

Dascalescu, L., Samuila, A., Dan, R., Iuga, A. and Morar, R. (1999). Multiple-Needle Corona Electrodes for Electrostatic Processes Application. *IEEE Trans. Ind. Appl.* 35: 543–548.

El-Mohandes, M.T., Ushiroda, S., Kajita, S., Kondo, Y. and Horii, K. (1992). Negative Corona in a Multiple Interacting Needle-to-Plane Gap in Air. *IEEE Trans. Ind. Appl.* IA-21: 518–522.

Huang, S.H. and Chen, C.C. (2001). Filtration Characteristics of a Miniature Electrostatic Precipitator. *Aerosol Sci. Technol.* 35: 792–804.

Kim, J.H., Yoo, H.J., Hwang, Y.S. and Kim H.G. (2012). Removal of Particulate Matter in a Tubular Wet Electrostatic Precipitator Using a Water Collection Electrode. *TheScientificWorld* 2012:532354, doi: 1100/2012/532354.

Kim, S.H., Sioutas, C. and Chang, M.C. (2000). Electrostatic Enhancement of the Collection Efficiency of Stainless Steel Fiber Filters. *Aerosol Sci. Technol.* 32: 197–213.

Kozlov, B.A. and Solovyov, V.I. (2005). Limit Current of a Multi-Needle Corona Discharge. *Tech. Phys.* 51: 821–826.

Lin, G.Y. and Tsai, C.J. (2010). Numerical Modeling of Nanoparticle Collection Efficiency of Single-Stage Wire-in-Plate Electrostatic Precipitators. *Aerosol Sci. Technol.* 44: 1122–1130.

Lin, G.Y., Chen, T.M. and Tsai, C.J. (2012a). A Modified Deutsch-Anderson Equation for Predicting Nanoparticle Efficiency by Electrostatic Precipitators. *Aerosol Air Qual. Res.* 12: 697–706.

Lin, G.Y., Le, T.C., Lu, W., Tsai, C.J., Chein, H.M. and Chang, F.T. (2013). High-Efficiency Wet Electrocyclone for Removing Fine and Nanosized Particles. *Sep. Purif. Technol.* 144: 99–107, doi: http://dx.doi.org/10.1016/j.seppur.2013.04.039.

Lin, W.Y., Chang, Y.Y., Syu, J.Y., Lu, S.H. and Chen, C.C. (2012b). Characterization of Charging Effects on

Different Particles and Discharge Electrodes, Abstract, EAC 2012, Spain.

Matts, S. and Öhnfeldt, P.O. (1964). Efficient Gas Cleaning with SF Electrostatic Precipitator. *Fläkt* 1: 93–110.

Mermelstein, J., Kim, S. and Sioutas, C. (2002). Electrostatically Enhanced Stainless Steel Filters: Effect of Filter Structure and Pore Size on Particle Removal. *Aerosol Sci. Technol.* 36: 62–75.

Ruttanachot, C., Tirawanichakul, T. and Tekasakul, P. (2011). Application of Electrostatic Precipitator in Collection of Smoke Aerosol Particles from Wood Combustion. *Aerosol Air Qual. Res.* 11: 90–98.

Sigmond, R.S. (1982). Simple Approximate Treatment of Unipolar Space Charge Dominated Coronas: The Warburg Law and the Saturation Current. *J. Appl. Phys.* 53*:* 891–898.

Sillanpää, M., Geller, M.D., Phuleria, H.C. and Sioutas, C. (2008). High Collection Efficiency Electrostatic Precipitator for in Vitro Cell Exposure to Concentrated Ambient Particulate Matter (PM). *J. Aerosol Sci.* 39: 335–347.

Thanh, L.C. (1985). Negative Corona in a Multiple Interacting Needle-to-Plane Gap in Air. *IEEE Trans. Ind. Appl.* IA-21: 518–522.

Received for review, May 5, 2013
Accepted, July 24, 2013